Stretchability study of conductive inks printed by Laser-induced forward transfer

Author: Eva Maria Torres Riera
*Facultat de Física, Universitat de Barcelona, Diagonal 645, 08028 Barcelona, Spain.**

Advisor: Juan Marcos Fernández Pradas

Abstract: Laser-induced forward transfer (LIFT) is a direct writing technique. As a nozzle-free method, it presents fewer constraints compared with other popular methods like inkjet printing. In this project, we analyze both morphological and electrical properties of the deposited material for three different inks, achieving a sheet resistance of 16 $m\Omega/\square$. Electrical properties under flexion are studied by applying deformation in a cantilever. Maximum relative deformations of 0.55% are possible before inducing irreversible damage in the electrical properties of the printed resistances.

I. INTRODUCTION

New material transfer techniques have been developed as a result of the increasing demand for smaller stretchable electronic devices [1]. Direct-write technologies have expanded in the past few years, with inkjet printing becoming the most widespread technique for printing devices. However, such techniques present considerable limitations in terms of both the viscosity of the ink and the size of the ink particles, since nozzles are required. Because of this, nozzle-free techniques, such as Laser-direct write techniques (LDW), present fewer constraints. The most widely used LDW approach is the laser-induced forward transfer (LIFT) [2].

LIFT is a versatile method of transferring materials from a carrier substrate coated with a donor layer to the receiver substrate [3]. The LIFT method is schematically represented in Fig. 1. The distance between the two substrates (donor and receiver), known as the gap, can be easily controlled and, when considering viscous inks, has a major effect on the parameters of the ink transfer [4]. If the gap distance and the laser pulse energy are adequate, some material from the donor layer is ejected and deposited on the receiving substrate placed in front of the donor layer. The deposition is promoted by a laser beam focused by a lens on the interface between the donor substrate and the donor layer. For this, the donor substrate must be transparent at the laser wavelength. An expanding bubble is created on the donor as a result of the laser energy absorption, and it expands to produce a jet that eventually reaches the receiver. Specifically, on high viscosity inks when the jet reaches the receiver, a bridge is formed and can remain for a long time [4].

In this work, the LIFT method is applied to inks with varying characteristics and parameters, and the aim is to compare both electrical characteristics and the behaviour of each ink when deformed.

*Electronic address: etorreri8@alumnes.ub.edu

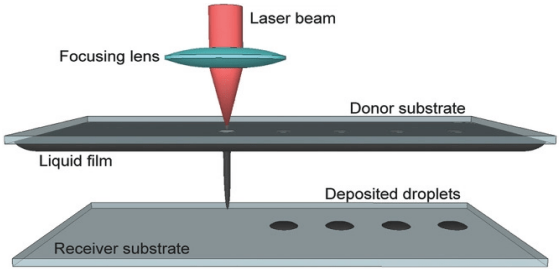

FIG. 1: Schematic representation of LIFT operation method. Image extracted from [3].

II. EXPERIMENTAL

A. Laser System

A Q-switched Ytterbium-doped fiber laser (Rofin Powerline F20 Varia) was used in the experiments presented. The device operates at the fundamental wavelength of 1064 nm and offers a variety of pulse duration. In this project, we used pulses of 4, 8, and 14 ns of duration. The laser system also contains two mirrors that deviate the laser beam along the x and y axes [5]. The allowed working area is 120 x 120 mm^2. Using the galvo head, any pattern can be marked at speeds ranging from 10 mm/s to 5 m/s. A lens of $f = 100\ mm$ was used to focus the laser beam. The laser beam has a Gaussian intensity profile and the beam power is linearly correlated with the pump power. The laser energy was used to characterize the irradiation conditions of study, but another important parameter is the fluence, which corresponds to the energy delivered per unit area. For Gaussian intensity profiles, the average fluence can be calculated by dividing the energy of a laser pulse (E_P) by the area of a circle with the beam waist as radius (w),

$$F_{av} = \frac{E_P}{\pi w^2} \tag{1}$$

where, in our experiments, $w = 20\ \mu m$.

The Visual Laser Marker program allows to adjust some laser beam parameters, such as the repetition rate

(2 kHz used in this experiment), the duration of the pulse, the speed of the beam or the separation of voxels centers. According to the pattern described at the program the scanning mirrors move in order to reproduce the arranged pattern.

B. Sample preparation and deposition

In the developed experiments, three different conductive pastes of silver (XTPL Ag nanopaste) nanoparticles have been studied. The properties of two of them are specified in Table I.

	XTPL CL60	**XTPL CL85**
% Solid content	60	85
Viscosity ($Pa \cdot s$)	$30 - 50$	> 100
Density (g/cm^3)	$1.85 - 2.50$	4.4
Electrical resistivity ($\Omega \cdot m$)	$5.11 \cdot 10^{-8}$	$4.2 \cdot 10^{-8}$

TABLE I: Portion of solid content, viscosity, density, and electrical resistivity of two of the different inks studied in this project.

The third ink considered in the project is XTPL *R&D*. Although not having its complete technical data sheet, solid content value is known to be 88.8%, and viscosity is estimated to be over $5 \cdot 10^6$ $Pa \cdot s$ by the supplier.

The donor substrate is prepared by manually spreading the ink inside a pool formed at the microscope slide, obtaining values of approximately 40 μm of thickness. Scotch tape is used for the pool's structure, with a thickness of 50 μm. As the donor layer is placed directly on top of the substrate, the gap between the donor layer and the receiver substrate is about 10 μm.

When the ink is deposited on the receiver substrate, it needs to be cured in order to improve its electrical properties. All three inks have been cured at the same temperature, $230°C$, during 20 minutes, as recommended in their technical data sheet.

C. Sample characterization

An optical microscope (Carl Zeiss, model AXiO Imager.A1) was used to analyze the morphology of the samples. The electrical sample was characterized using a multimeter (Aim-TTi, model 1906) through the two-point method. In order to characterize the electric properties under flexion of each ink, printing has been done on PowerCoat Energizing paper, by Arjowiggins, and the multimeter mentioned has been used to measure the variation of resistance.

III. RESULTS AND DISCUSSION

A. Droplets size study

The study first explores the morphology of the deposited voxels at various energies and for each ink examined. Considering the different fluidic properties of the inks tested, the energy required to get droplets varies significantly and so does their size. Experimental results presented in Fig.2 indicate that, for each ink, a larger energy results in a larger voxel radius, as it was expected since Breckenfeld et al [6]. It is worth mentioning that squared and cube voxel radius present a quite linear correlation with the applied energy. Additionally, it is important to observe the different values of the threshold energy, i.e. the minimum energy required to print the droplets. For energies below the threshold value, the bubble cannot reach the receiver layer and returns to the donor substrate. The experiments also demonstrate that the higher the viscosity of the printing liquid, the higher the energy required to generate a droplet.

Upon analysis, it has been determined that the minimum energy required to deposit droplets of XTPL CL60 ink is (8.9 ± 0.5) μJ producing voxels with radii of (60.9 ± 0.3) μm. Regarding the XTPL CL85, the minimum energy is (17.1 ± 0.5) μJ generating voxels with average radii of (14.1 ± 0.3) μm; and for the XTPL RD ink (43.4 ± 0.5) μJ generates voxels with (30.7 ± 0.3) μm of radius.

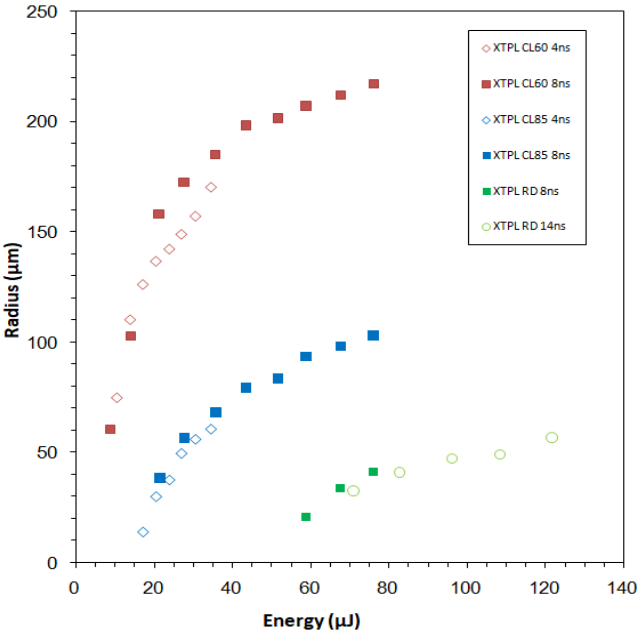

FIG. 2: Radius of deposited voxels at different energies for XTPL CL60 ink, in red; XTPL CL85, in blue; and XTPL *R&d* in green. Radius uncertainty is 10 μm and energy uncertainty is 0.5 μJ.

B. Printing of lines

Continuous lines are formed by overlapping single dots, i.e, by reducing the distance between the center of contiguous voxels. In this study, the main objective is to determine the optimal line printing conditions for each of the inks to obtain the lowest sheet resistance. Since diverse cases are being considered with different applied energies, higher energy will result, typically, in a larger droplet, which leads to larger line widths. Additionally, it is important to mention that the width of the lines usually, for fixed energy, remains constant regardless of the overlap.

In this work each ink is analyzed individually in order to determine its optimum line printing conditions. However, some analog behaviors between all of them are observed. Firstly, there is a threshold overlap value, which may differ for each ink. According to *Sopeña et al.* [4], when overlapping voxels of a non-Newtonian ink to obtain continuous lines, the spot distance must be equal or greater than the maximum bubble radius formed by the laser pulse on the donor layer. Otherwise, there would be a strong interaction between the bubbles, resulting in a discontinuous transfer of the layer. This would explain that for very low values of voxel separation, such as 0.5 μm, the maximum overlap of the voxels allowed by the program, a *splash* phenomenon is observed. This phenomenon may be due to the impact of successive pulses in a short time and space interval, which could create a bubble that breaks and spreads in all directions.

The most representative cases of the conditions mentioned, for the inks described, are represented in Fig. 3.

First, XTPL CL60 ink is considered. With a pulse duration of 4 ns and applying pulse energy of (13.8 ± 0.5) μJ uniform lines are formed at spot distances of 90 μm and 80 μm. At this applied energy, lines width presents values of (250 ± 10) μm. When (27.2 ± 0.5) μJ are applied, the lines are formed at spots distances ranging from 100 to 70 μm, resulting in lines width of (517 ± 10) μm. With 8 ns, if the energy is (8.9 ± 0.5) μJ, lines form almost at every spot distance ranging from 100 μm to 60 μm. With the energy set to $(14.5 \pm 0.5) \mu J$, spots distances of 100, 90 and 80 μm cause uniform lines, while smaller distances cause almost uniform lines, but with a significant *splash* effect.

Secondly, we consider the XTPL CL85 ink, and by varying the overlap of the voxels, we can observe that, for 4 ns of pulse duration and energy of (20.4 ± 0.5) μJ, continuous lines are formed when the spot distance reaches 80 μm. In the case of voxel separations of 60 μm or less, the non-continuous line phenomenon is observed. The line width values obtained at this applied energy are of (80 ± 10) μm. When the energy of (23.9 ± 0.5) μJ is considered, the results indicate that continuous uniform lines, with a width of (88 ± 10) μm, form at a spot distance of 70 μm. Lower values of spot distances also result in non uniform lines under these conditions. With a pulse duration of 8 ns, at an energy of (8.9 ± 0.5) μJ, it is observed that uniform continuous lines occur when the spot distance reaches 80 μm. In the case of higher energy, (14.1 ± 0.5) μJ, lines form in spot distances of 80, 70, and 60 μm. The reason for this may be that higher energy facilitates ink transfer, and since it also enlarges voxels, the conditions for creating lines are favored.

Lastly, we examined the XTPL *R&D* ink. As expected, since the viscosity was higher than the other inks, it was harder to achieve uniform continuous lines, so a higher energy is required. Although the difficulty, uniform continuous lines are formed at pulse duration of 14 ns and at energies of (70.9 ± 0.5) μJ and (82.5 ± 0.5) μJ, when spots distances reach values of 70 and 60 μm. When (82.5 ± 0.5) μJ are applied, we obtain lines with a width of (90 ± 10) μm.

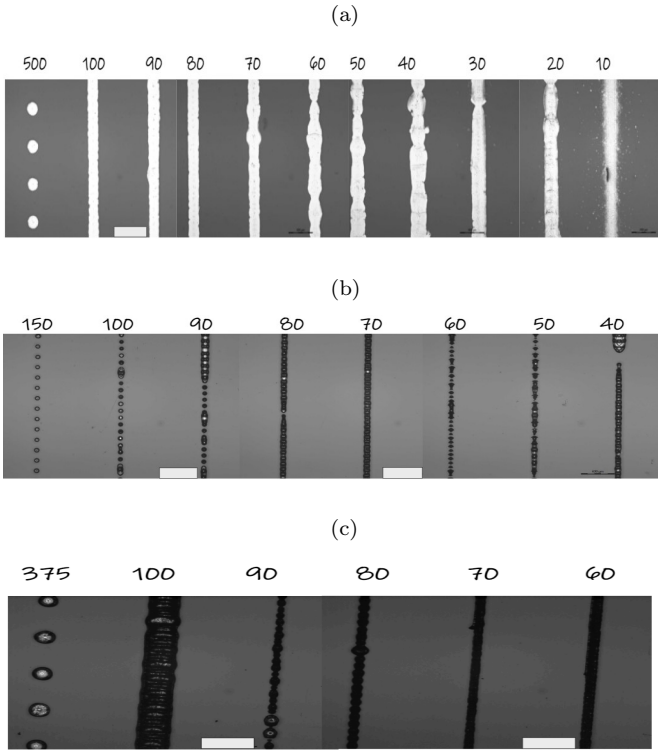

FIG. 3: Optical images showing lines printed with (a)XTPL CL60 with energy of (13.8 ± 0.5) μJ ; (b) XTPL CL85, at 4ns and (20.4 ± 0.5) μJ; (c) XTPL *R&D* at 14 ns, with energy of (82.5 ± 0.5) μJ. Separation of voxels centers is specified above lines in µm. Scale bar corresponds to 400 μm.

C. Sheet Resistance Results

The conductivity is the reciprocal of resistivity. The sheet resistance was included in the analysis even though the physical parameter being measured is the resistance, since removing the influence of the geometric factor in a planar sample will provide a better comparison between

samples. To do so, we use formula (2).

$$R_s = R\frac{W}{L} \tag{2}$$

where R is the resistance, W is the width and L is the length.

In this work we provide the minimum sheet resistance measured for each ink, after determining its optimum conditions of energy and spot distance.

After careful examination, the sheet resistance of the optimal deposited lines for each ink has been established to be: $Rs = (40\pm1)\ m\Omega/\square$ for XTPL CL60; $Rs = (21.3\pm 0.5)\ m\Omega/\square$ for XTPL CL85 ; and $Rs = (16 \pm 2)\ m\Omega/\square$ for XTPL $R\&D$.

It was expected that XTPL $R\&D$ ink would present the lowest sheet resistance out of the three inks. XTPL CL85 sheet resistance was also expected to be lower than the value for XTPL CL60 ink, since the sheet resistance is a parameter indirectly proportional to the thickness of the deposited material, which is also related to the amount of solid content of the ink. Specifically, the higher the number of nanoparticles of Ag that the ink has, i.e, the higher the solid content, more material is most likely to be transferred to the receiver donor.

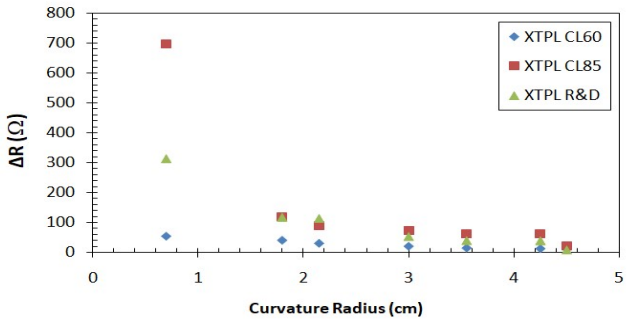

FIG. 4: Plot of the variation of resistance versus the radius of the cylinder. Resistance uncertainty is 2 Ω, for XTPL CL60, 5 Ω for XTPL $R\&D$ and XTPL CL85, for high values of curvature radii, and 20 Ω, for the value corresponding to the smallest cylinder's radius. Curvature radius uncertainty is 0.1 cm.

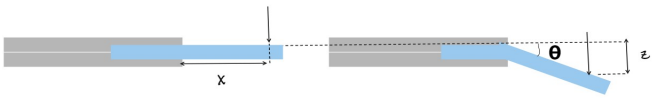

FIG. 5: Schematic representation of the process of causing the samples to bend.

D. Flexibility study

In this project, in order to characterize the electrical properties under flexion of each ink, two different methods have been implemented. The first technique consists of measuring variations of resistance when the sample is wrapped around several cylinders with different diameters, as proposed in [7]. The second method, which has allowed determining the variation of resistance as a function of the angle of flexion is based on the deformation caused in a cantilever. The samples are placed on top, so they are always subject to stretching.

The aim of the first method is to determine the change of resistance when deforming the sample. In this case, as the radius of the cylinder reduces the resistance increases, as shown in Fig. 4. The results of this experiment show that XTPL CL85 ink presents a higher variation of resistance whilst XTPL CL60 experiments the lowest change. Although this first technique allows a qualitative analysis of the variation of resistance when deforming the sample, the deformation caused is important enough to have suppressed any possibility to recover the initial values of resistance when deformation is no longer applied.

The second method, which can induce smaller deformations, has allowed to determine the conditions under which reversibility can occur, i.e. to obtain the initial resistance values after removing the deformation. By controlling the distance between the load applied and the support point of the sample and the lineal deformation caused by the load, the angle of flexion can be easily computed (as shown in Fig. 5). By applying the cantilever and measuring the variation of resistance, we observe that the higher angle of flexion, the higher the deformation induced in the samples, and consequently, a higher variation of resistance is measured. As shown in Fig.6, all three inks considered present a nonlinear correlation between the increase of resistance and the deformation induced. Plots in Fig.6 also exhibit a significant increase in the resistance for a certain angle of flexion, angle in which the resistance begins to increase faster, until it reaches really high values of resistance. When carrying out the experiment, one of the main objectives was to determine whether the deformation induced in the samples was reversible or not, i.e, if it presented hysteresis. For all three inks, it was concluded that when small deformation was caused, low value of angle of flexion, the sample if returned to the original state, would eventually return to the value of resistance obtained for null deformation. However, when increasing the deformation produced, the process becomes irreversible, since although the resistance decreases after eliminating the cause of the deformation, the final obtained value is significantly higher than the initial value measured. This is probably due to the formation of cracks produced by the sample stretching.

A parameter useful to characterize the range of angles of flexion where the increase of resistance caused by the deformation is reversible is given by the relative deformation $\frac{\Delta l}{l}$, which can be calculated by $\frac{\Delta l}{l} = \frac{2d}{\varrho}$ where $d = (230 \pm 5)\ \mu m$ is the thickness of the paper deformed and ϱ corresponds to a parameter that characterizes the deformation, since it depends on the distance between the support and the applied load, the distance at which the resistance is measured and the angle of flexion.

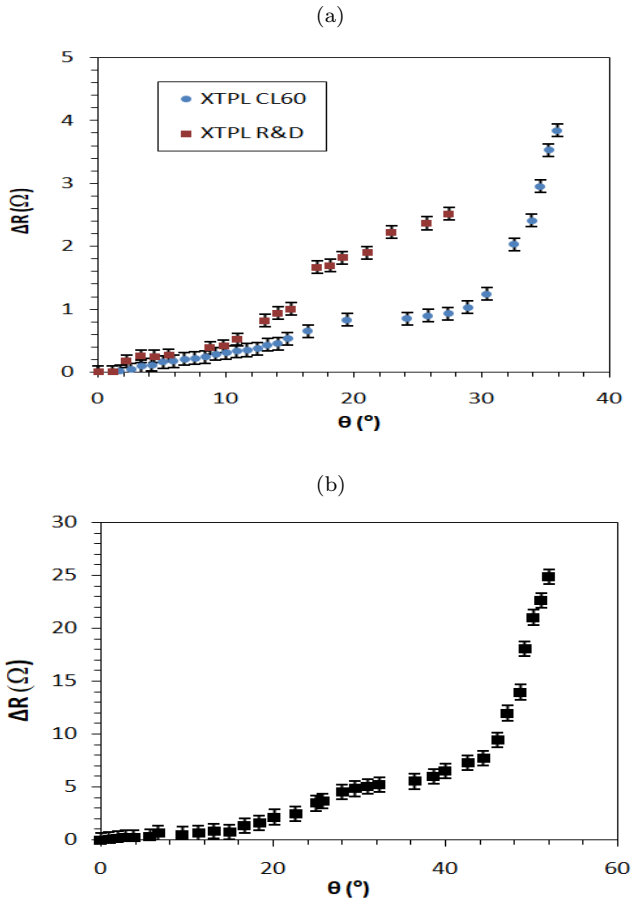

FIG. 6: Plots showing the variation of resistance versus the angle of flexion that characterizes the deformation for (a)XTPL CL60 and XTPL *R&D* and (b) XTPL CL85 ink.

When comparing all three inks, XTPL CL85 presented a higher value of flexion angle for which the resistance increased drastically, $\theta \approx 40°$ which corresponds to a curvature radius of approximately (20 ± 0.5) cm, which causes a maximum relative deformation of 0.55%. In the case of XTPL CL60, the threshold angle is $\theta \approx 20°$, corresponding to a (28.8 ± 0.5) cm radius of curvature, and consequently to a maximum relative deformation of 0.31%. Lastly, XTPL *R&D* presents irreversibility for angles above $\theta \approx 12°$, i.e, a radius of curvature of (26.6 ± 0.5) cm, corresponding to a maximum relative deformation of 0.41%.

If flexibility is the only parameter considered, the XTPL CL85 would be the most suitable, since it can be deformed much more than the other two inks considered. Furthermore, it presents the highest range of variation of resistance, which could become useful on different applications, such as sensors.

IV. CONCLUSIONS

- The LIFT technique has been proven to be adequate for the printing of conductive nanoinks of high viscosity, taking into account that the higher the viscosity of the ink, the higher energy of the laser beam is needed to print voxels.
- Under optimum conditions, smallest sheet resistance obtained is $Rs = (16 \pm 2)$ $m\Omega/\square$ with XTPL *R&D*, the ink with higher solid content.
- The higher the induced deformation, the least likely is to recover the initial conditions, as it becomes an irreversible process for larger angles of flexion. XTPL CL85 ink presents higher flexibility than XTPL CL60 and XTPL *R&D* as it can be deformed for larger angles of flexion, in particular, it presents a maximum relative deformation of 0.55%. Also, since it presents a larger variation of resistance, it can be used as a sensor.

Acknowledgments

I would like to thank my advisor Dr. Juan Marcos Fernández Pradas for his help and lending of the equipment. I also acknowledge my laboratory colleague E. Martí for the advice and help at the laboratory. Many thanks specially to my family and friends for the wholehearted support throughout all these years.

[1] Stewart, B. G., Sitaraman, S. K. (2021). Biaxial inflation stretch test for flexible electronics. Advanced Engineering Materials, 23(6), 2001503.
[2] Fernández-Pradas, J. M., Serra, P. (2020). Laser-induced forward transfer: a method for printing functional inks. Crystals, 10(8), 651.
[3] Serra, P., Piqué, A. (2019). Laser-induced forward transfer: Fundamentals and Applications. Advanced Materials Technologies, 4(1), 1800099.
[4] Sopeña, P., Fernández-Pradas, J. M., Serra, P. (2020). Laser-induced forward transfer of conductive screen-printing inks. Applied Surface Science, 507, 145047.
[5] Paniagua Seriols, P. (2019). Characterization of a fiber laser system for materials processing. (TFG, University of Barcelona)
[6] Breckenfeld, E., Kim, H., Auyeung, R. C., Piqué, A. (2016). Laser-induced forward transfer of Ag nanopaste. JoVE (Journal of Visualized Experiments), 109, e53728.
[7] Chen, Y., Munoz-Martin, D., Morales, M., Molpeceres, C., Sánchez-Cortezon, E., Murillo-Gutierrez, J. (2016). Laser induced forward transfer of high viscosity silver paste for new metallization methods in photovoltaic and flexible electronics industry. Physics Procedia, 83, 204-210.